Planetary and Space Science 102 (2014) 35–44

Contents lists available at ScienceDirect

Planetary and Space Science

journal homepage: www.elsevier.com/locate/pss

Martian satellite orbits and ephemerides

R.A. Jacobson [a,*], V. Lainey [b]

[a] Jet Propulsion Laboratory, California Institute of Technology, 4800 Oak Grove Drive, Pasadena, California, USA
[b] Institut de Mécanique Céleste et de Calcul des Ephémérides, Observatoire de Paris, UMR 8028 du CNRS, UPMC, 77 Av. Denfert-Rochereau, 75014 Paris, France

ARTICLE INFO

Article history:
Received 14 December 2012
Received in revised form
6 May 2013
Accepted 10 June 2013
Available online 18 June 2013

Keywords:
Phobos
Deimos
Mars
Planetary satellites
Orbits

ABSTRACT

We discuss the general characteristics of the orbits of the Martian satellites, Phobos and Deimos. We provide a concise review of the various descriptions of the orbits by both analytical theories and direct numerical integrations of their equations of motion. After summarizing the observational data used to determine the orbits, we discuss the results of our latest orbits obtained from a least squares fit to the data.

1. General orbital characteristics

The orbits of Phobos and Deimos are slightly inclined to the Martian equator; the Deimos orbit is nearly circular but the Phobos orbit has a small but significant eccentricity. The motion of both satellites is direct, i.e., in the same direction as the rotation of Mars. If Mars and its satellites were spherically symmetric and we viewed Mars and each satellite as an isolated system, the satellites would move along elliptical orbits as dictated by Kepler's laws of planetary motion. In reality, however, the elliptic motion is perturbed by additional gravitational forces acting on the satellites primarily due to: (1) the aspherical Martian gravity field, (2) the Sun, (3) the planets and asteroids, (4) the tides raised on Mars by the satellites and the Sun, (5) the mutual attraction of the satellites, (6) the aspherical gravity fields of the satellites themselves including the raised on the satellites by Mars and the Sun.

The dominant perturbations are from the Martian gravity field and the Sun; the remaining perturbations are quite small. The Mars oblateness causes the orbit planes to precess in a retrograde direction about the Mars pole, and the Sun's attraction causes a retrograde precession of the orbit planes about the normal to the Mars orbit. For each satellite the net precession is retrograde about the normal to its Laplace plane, a plane lying between the Mars equator and Mars orbit; to a first approximation, the satellite orbits maintain constant inclinations to the Laplace planes. Fig. 1 displays various planes and angles associated with the orbits. The inclination and node of the Mars orbit referred to the ecliptic are i' and Ω', respectively, with the latter being measured from the intersection of the ecliptic with the reference plane of the International Celestial Reference Frame (ICRF). The precession angle P and obliquity Q orient the Mars equator with respect to the Mars orbit, and P and I′ define the Laplace plane with respect to the Mars orbit (the Laplace plane and Mars equator share a common node on the Mars orbit). Finally, Ω is the node of the satellite orbit on the Laplace plane and i is the inclination to that plane. The combined Mars oblateness and solar attraction also induce a secular advance of the lines of apsides of each orbit at a rate near the precession rate. Almost all periodic orbital perturbations are small, the exception being a large (110 km) long period perturbation (54.8 years) in the Deimos mean longitude due to a combined effect of the Sun and the Martian gravity field.

The Phobos orbital period is less than the Mars rotation period, i.e., Phobos is well within the Mars synchronous orbital radius (where a satellite's orbital period equals the planet's rotation rate); Deimos, on the other hand, lies beyond the synchronous orbit. Consequently, the tide raised on Mars by Phobos causes Phobos to accelerate, but the tide raised by Deimos causes Deimos to decelerate. The tidal effect on Phobos has been observationally detected, but the effect on Deimos has not as yet.

Because of its irregular shape and eccentric orbit, Phobos is subject to a gravitational torque exerted by Mars. Consequently, its rotational motion includes a forced oscillation primarily in the longitude direction. The Phobos gravity field and libration introduce secular and periodic perturbations into its orbital motion; the

* Corresponding author. Tel.: +1 8183547201; fax: +1 8183545904.
E-mail address: robert.jacobson@jpl.nasa.gov (R.A. Jacobson).

0032-0633/$ - see front matter © 2013 Elsevier Ltd. All rights reserved.
http://dx.doi.org/10.1016/j.pss.2013.06.003

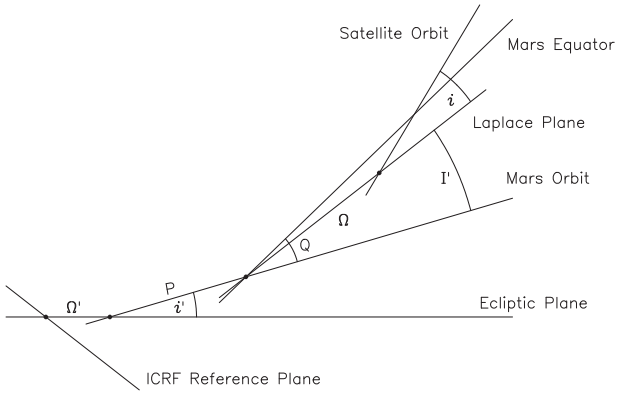

Fig. 1. Satellite orbital geometry.

dominant effect being a decrease in the periapsis precession rate. In principle, Deimos is also subject to similar perturbations, but its less eccentric and more distant orbit mitigate the effect of its gravity field.

2. Review of analytical theories

2.1. Struve theory

Struve (1911) developed one of the first analytical theories for the description of the satellites' orbital motion. The theory places each satellite in an elliptical orbit but accounts for the secular perturbation due to the Mars oblateness and the Sun by allowing the pericenter longitude, ϖ, to precess in the orbit plane and the ascending node, Ω, to precess about the normal to the satellite's Laplace plane; the orbital inclination, i, to the Laplace plane was constant as was the eccentricity of the ellipse, e. The mean motions, n, along the orbits and the orbital semimajor axes, a, were treated as independent parameters; since the orbits are perturbed conics, their mean motions and semimajor axes do not satisfy Kepler's third law. Struve determined the mean longitudes of the satellites, λ, the elements $(a, e, i, \varpi, \Omega)$, the mean motions, and the precession rates $(\dot{\varpi}, \dot{\Omega})$ for Julian Date 2413102.0 by fitting his theory to Earthbased astrometric observations spanning the years 1877–1909. The ephemerides in *The Astronomical Ephemeris* were based on this theory (Wilkins and Springett, 1961). Burton (1929) updated the values of the elements by including in the fit astrometry obtained at the U.S. Naval Observatory in 1909, 1924, and 1926, and Wilkins (1966) later extended the data arc to 1928. Shor (1975) revised the theory by adding an acceleration term to the mean orbital longitudes to account for the tidal acceleration; he estimated the elements, precession rates, and the acceleration with data from 1877 to 1973.

2.2. Sinclair theory

Sinclair (1972) developed a dynamical theory using the method of the variation of arbitrary constants (Brouwer and Clemence, 1961) to obtain an approximate analytical solution to the satellites' equations of motion. Those equations accounted for the point mass gravitational attraction of Mars and the Sun and the effects of the Mars oblateness and the precession of the equator of Mars (a consequence of the solar torque acting on Mars). Tidal forces were not included, but empirical acceleration corrections were added to the satellites' longitudes. The theory took the form of secular and periodic corrections to the elements $(a, e, \lambda, \varpi, \Omega)$ and to the sine of the inclination of the satellite's orbit to the Laplace plane. The fundamental parameters in the theory were the epoch values elements of the orbits, the mean longitude accelerations, the mass of Mars, the second, third, and fourth zonal harmonics in the Martian gravity field, and the orientation of the Martian pole. The theory provided analytical expressions for mean motions and periapsis and node precession rates as function of the parameters. Sinclair determined the parameters via a fit to observations over 1877–1969, but he concluded that the data were insufficient to conclusively determine the longitude accelerations, the Mars equator precession rate, and any zonal harmonics higher than second degree. Ephemerides derived from the theory replaced the Struve ephemerides in the *The Astronomical Ephemeris* (Seidelmann, 1992).

Sinclair's original theory did not include the long period term in the Deimos mean longitude. That term was overlooked until Born and Duxbury (1975) found that it was needed in order to properly process the imaging data from *Mariner 9*. Sinclair (1978) added the term and extended his data fit to Earthbased data through 1973 and the imaging data from *Mariner 9*. Like Shor, he obtained an estimate of the Phobos longitude acceleration. Sinclair (1989) expanded the theory with some additional periodic terms and redetermined the theory parameters adding to his data set Earthbased data to 1988 and the imaging data from *Viking*. Jacobson et al. (1989) performed an independent analysis with Sinclair's theory and observations.

Morley (1989b, 1990) revised the basic Sinclair theory increasing its accuracy with more terms including some of second order. The revision was motivated by a need to compute high precision orbits in support of the Soviet *Phobos 2* mission. Morley's revision included all periodic perturbations with amplitudes greater than 25 m and was verified, via comparison with numerical integration, to have an overall accuracy of 100 m in the Mars relative satellite positions over a 60 day interval, which was sufficient for the mission. The theory was fit to the complete set of Earthbased (1877–1988), *Mariner 9* and *Viking* observations.

2.3. Adaptations of artificial satellite theories

With the advent of artificial satellites of the Earth a number of analytical theories were developed to describe their orbital motion; a classic among these is the theory of Brouwer (1959). Because the Martian satellites are small, it was found that these theories could be adapted as models for their orbits. Unlike the theories of Struve or Sinclair, those based on the artificial satellite approach used the Mars equator, not the Laplace plane, as the reference plane.

Aksnes (1972) developed a theory which accounted for secular and periodic perturbations from the zonal harmonics of the Mars gravity field and was expressed in terms of Hill variables $(r, \dot{r}, u, \Omega, G, H)$: r is the distance of the satellite from Mars in the satellite orbital plane, $\dot{r}$ is the radial velocity in the satellite orbital plane, u is the argument of latitude, $G = \sqrt{\mu a(1-e^2)}$, where μ is the Newtonian gravitational parameter of Mars, $H = G \cos i$. The theory was used to support the early phase of the *Mariner 9* mission. However, it proved inadequate for the analysis of *Mariner 9* imaging data and was replaced by the theory of Born and Tapley (1969) and Born and Duxbury (1975). The Born theory contained additional terms for the perturbations due to Mars gravity and the Sun and was the first to account for the long period Deimos perturbation. It described the satellite motion using the set of nonsingular elements: a, $h = e \sin \varpi$, $k = e \cos \varpi$, λ, $p = \sin i \sin \Omega$, $q = \sin i \cos \Omega$.

Ivanov et al. (1988) and Kudryavtsev (1993) developed a high precision semi-analytical theory for planetary satellites that represented the osculating orbital elements $(a, e, i, \lambda, \varpi, \Omega)$ referred to the planet equator as a time series. (A semi-analytical theory is one in which some terms are specified numerically based on

assumed values for the theory parameters rather than analytically as a function of the parameters themselves.) Applied to the Martian satellites, the theory accounted for the secular and periodic perturbations from the Mars gravity field and the Sun but was extended to include second order terms as well as the Phobos longitude acceleration. The theory was fit to Earthbased (1877–1986), *Mariner 9*, and *Viking* observations and was used in the navigation of the Soviet *Phobos 2* mission (Kolyuka et al., 1991b). After the mission ended the fit was updated with Earth-based data through 1988 and the *Phobos 2* imaging.

As with the above theory, the semi-analytical theory of Emelyanov (1986), Emelyanov and Nasonova (1989), Emelyanov et al. (1993) employed osculating orbital elements and modeled the effects of the Mars gravity field, the Sun, and the Phobos longitude acceleration, but it also included secular perturbations on the Phobos orbit due to the Phobos gravity field. The theory was fit to Earthbased data (1877–1989) and the *Mariner 9*, *Viking*, and *Phobos 2* imaging.

Finally, although Wnuk and Breiter (1992) did not develop a specific theory, they carried out an informative examination of the possibility of adapting artificial satellite theories to Mars for both spacecraft and satellites. They quantified the perturbations of the Mars gravity potential to determine which terms needed to be included in any theory.

2.4. Chapront-Touzé theory

The theory of Chapront-Touzé (1988, 1990a,b) is a high precision semi-analytical one that models the perturbative effects of the Sun and planets, the Martian gravity field, the mutual perturbations of Phobos and Deimos, and the perturbations due to the gravity field of Phobos. The longitude acceleration of Phobos is included as a parameter, but tides are not explicitly modelled. The theory also takes into account the precession and nutation of the Mars equator and the libration of Phobos; the model for the latter was adapted from the work of Borderies and Yoder (1990). Unlike previous theories, orbital elements are not used; instead, the theory provides the satellite Cartesian coordinates and their velocities in the Mars equator of date coordinate system. The theory was designed to have an internal precision of a few meters in Mars relative positions over 20 years and was developed to support scientific data analysis for the Soviet *Phobos 2* mission. However, due to an onboard computer malfunction, the *Phobos 2* spacecraft failed to carry out the third stage of its mission. In that stage, the spacecraft was to approach to within 50 m of Phobos, make high-resolution observations of its surface, and deploy a lander. Because of the spacecraft failure, no data analysis was done, and the satellite orbit theory was not needed. Ultimately, ephemerides were produced based a fit of the theory to Earth-based astrometry (1877–1988) and the *Mariner 9*, and *Viking*, and *Phobos 2* imaging data (acquired prior to the spacecraft failure). Unfortunately, because of the semi-analytical nature of the theory, it is difficult to revise in light of new observations or new values for fundamental constants such as the coefficients in the Mars or Phobos gravity fields, i.e., the numerical terms would have to be regenerated. There have been no published updates to the theory.

3. Review of numerical integrations

The first use of a numerically integrated Phobos ephemeris was by Tolson et al. (1977) in his analysis of the Viking spacecraft Doppler and range tracking data to determine the mass of Phobos. He needed an integrated ephemeris because none of the theories existing at that time were of sufficient precision for his purposes. Tolson provided no details as to the dynamical model used in his integration; however, he did state that the Viking spacecraft was integrated together with Phobos and that his integration technique employed a power series algorithm (Hartwell, 1967). We assume that his model was sufficiently complete to be able to produce a spacecraft orbit of an accuracy compatible with the tracking data. To obtain the Phobos orbit he did not fit his integration to observations but rather to positions derived from the theory of Born and Duxbury (1975) over the time span of his data analysis. Consequently, his orbit would have matched Born's in the mean but would have different and more accurate periodic perturbations.

Lainey et al. (2007) developed the first complete numerically integrated ephemeris for the satellites. His force model included a 10th degree and order aspherical Martian gravity field (Tyler et al., 2003), perturbations due to the Sun, Jupiter, Saturn, Earth, and Moon, the mutual perturbations of the satellites, the effects of tides raised on Mars by both satellites, and the quadrupole moments of the Phobos gravity field (the Phobos figure). Unlike the previously described theories that used orbital elements, Lainey's integration was carried out in planetocentric Cartesian coordinates referred to the J2000 inertial reference frame. His integration routine was based on the method of Gauss–Radau polynomials (Everhart, 1985) with a constant step size of 2160 s; his estimated accuracy was a few hundreds of meters in Mars relative positions over a century. The orbits were fit to Earthbased observations and the spacecraft based observations from *Mariner 9*, *Viking*, *Phobos 2*, *Mars Global Surveyor*, and *Mars Express*; the data arc spanned 1877–2005.

To support the planned Russian *Phobos-Grunt* mission, Akim et al. (2007) and Shishov (2008) also numerically integrated the orbits of the satellites. Their force model was analogous to Lainey's, but they restricted the Martian gravity field (Lemoine et al., 2001) to eighth degree and order and did not include tidal perturbations. Unlike Lainey their motion was computed using Lagrange's equations for the evolution of the osculating orbital elements (Brouwer and Clemence, 1961), and the Phobos longitude acceleration was implemented as a correction term to the longitude. No details are available as to the integration procedure used. The orbits were determined by fitting the Earthbased astrometry over 1877–1989, the spacecraft observations from *Mariner 9*, *Viking*, *Phobos 2*, *Mars Global Surveyor*, and *Mars Express*, the solar relative positions of Phobos seen from the Martian landers *Spirit* and *Opportunity*, and the MOLA ranging data to Phobos from *Mars Global Surveyor*. The *Phobos 2* and *Mars Global Surveyor* spacecraft tracking data were also processed to obtain spacecraft–Phobos relative positions and to estimate the Phobos mass.

Jacobson (2010) repeated and extended the work of Lainey. He ignored the effect of the tide raised on Mars by Deimos (it is extremely small and was considered unobservable at the time), but he included the libration of Phobos in the Phobos gravity model. The Mars gravity field (Konopliv et al., 2006) was limited to degree 8 in the zonal gravity harmonics and degree and order 5 in the tesserals (higher degrees have a negligible effect on the satellite orbits). Like Lainey he employed Cartesian coordinates but in the ICRF and referred to the center of mass of the Martian planetary system composed of Mars and its two satellites. His integration algorithm was a Gauss–Jackson method (Jackson, 1924) modified to automatically select the order and step size of the integration to satisfy a local error tolerance on velocity; the error tolerance used was 1×10^{-12} km/s which resulted in a 15th order integration with a step size of 256 s. The orbit fit used all Earth-based and spacecraft based observations from 1877 to 2007; among them were additional *Mars Express* imaging and imaging from *Mars Reconnaissance Orbiter*. Also included in the data set were the Doppler tracking data from the *Viking* and *Phobos 2*

spacecraft. These data provided information on the masses of Phobos and Deimos as well as their positions at the times of the spacecraft flybys. Additional parameters in the fit were the satellite masses and the amplitude of the Phobos libration, which has a direct effect on the Phobos quadrupole acceleration.

4. Observational data

4.1. Earthbased data

As discussed by Pascu et al. (2014) the satellites are difficult to observe because they are faint, fast moving, and lie close to the bright planet. Nevertheless, a large number of astrometric measurements have been collected over the years since their discovery. These are primarily positions of the satellites relative to Mars or to each other observed visually, photographically, or with a CCD. The visual measurements were corrupted by errors due to: (1) the large magnitude differences between planet and satellites, (2) the large diameter of the planet (which made the determination of its center difficult), (3) the bright halo around the planet, (4) the rapid motion of the planet and satellites. The advent of photography and later the introduction of the CCD reduced the measurement errors and improved their time resolution.

Morley (1989a) compiled a catalog of the astrometric observations acquired during the years 1877–1982. The catalog was designed to be the source of data for ephemeris production in support of the Soviet *Phobos Mission*. Morley provided a short history of the observations, put them all on the Coordinated Universal Time (UTC) timescale, corrected obvious blunders, performed an accuracy analysis, and commented on a number of the data sets. His work has been a valuable guide for the use of the observations in modern ephemeris development. Most of the data in the catalog can also be found in the Natural Satellites Astrometric Database (NSDB) (Arlot and Emelyanov, 2009) maintained jointly by the Sternberg Institute and the Institut de Méchanique Céleste et de Calcul des Ephémérides. The NSDB is also a good source for post-1982 astrometry, particularly the large set of observations made in 1988 in connection with the *Phobos Mission*. In recent years some of the old photographic astrometry in Morley's catalog has been re-reduced with modern techniques; these data are also available from the NSDB.

4.2. Spacecraft data

Mariner 9 was the first spacecraft mission to use imaging observations from a spacecraft to help navigation. These images, which were acquired with the onboard science camera, contained the satellites against a stellar background and, when reduced, provided absolute positions of the satellites as viewed from the spacecraft (Duxbury and Callahan, 1989); they were analogous to the absolute photographic astrometry obtained from the Earth. Because the satellites are in orbit about Mars, the positions gave the spacecraft navigators indirect measures of the spacecraft positions relative to Mars. These were critical measurements because, although the spacecraft positions relative to the Earth could be determined accurately from tracking data, the position of Mars relative to the Earth was not well enough known. Consequently, the accuracy of the Mars relative positions of the spacecraft, as determined by tracking, were limited by the Mars ephemeris error. The astrometry from *Mariner 9* gave satellite positions relative to Mars accurate to better than 10 km (roughly equivalent to 0.″025 from the Earth). The *Viking* mission continued the use of optical navigation, obtaining spacecraft based satellite astrometry comparable to that from *Mariner 9* (Duxbury and Callahan, 1988).

Because of improvements in the ephemeris of Mars, optical navigation was not needed to guide the *Mars Reconnaissance Orbiter* spacecraft into Martian orbit. However, rather than eliminate optical navigation entirely, the *Mars Reconnaissance Orbiter* Project permitted the spacecraft, on its approach to Mars, to be used as a test bed for a new dedicated optical navigation camera (Synnott, 2007) (on all previous spacecraft missions the science camera had been used for optical navigation). The data from this test yielded a large number of Phobos and Deimos astrometric positions accurate to 7 and 5 km, respectively.

During the Soviet *Phobos 2* a series of imaging observations of Phobos and Deimos from the spacecraft were acquired expressly for the purpose of providing astrometric data to support dynamical studies (Kolyuka et al., 1991a). These had astrometric position accuracies of 2 km for Phobos and 10 km for Deimos. Similarly, a series of observations were made with the *Mars Express* Super Resolution Channel (SRC) framing camera to obtain astrometric positions of the satellites. Oberst et al. (2006) report on the initial series in 2004–2005, which yielded Phobos and Deimos astrometric positions accurate to 2 and 5 km, respectively. Willner et al. (2008) provided additional Phobos observations acquired between 2004 and 2007, which were reduced with an improved technique and provided astrometric positions having an accuracy of 0.5 km, and Pasewaldt et al. (2011) contributed additional Deimos astrometry with position accuracies in the 1–3 km range.

Besides imaging observations, a number of other types of satellite measurements have been made involving spacecraft. Thomas et al. (1999) derived a correction to the Phobos position from the measurement of the time of egress of Phobos from an eclipse seen by the Imager on the *Mars Pathfinder* spacecraft. A Phobos position correction was obtained by Banerdt and Neumann (2000) from ranging between the *Mars Global Surveyor* spacecraft and Phobos acquired with the Mars Orbiter Laser Altimeter (MOLA). MOLA was also used to observe transits of the shadow of Phobos across the Martian surface (Bills et al., 2005), and Phobos and Deimos transits across the solar disk were seen by the *Mars Exploration Rovers* (Bell et al., 2005).

The tracking data of spacecraft in the vicinity of the satellites are also crucial to the determination of the satellite orbits. These data provide a direct measurement of the masses, which are needed to model the mutual satellite interactions. Moreover, the data add indirect constraints on the satellite positions during the close encounters with the spacecraft. For more details concerning the use of spacecraft tracking see Pätzold et al. (2014). Doppler tracking is available from the *Viking* 1 and *Viking* 2 (Snyder, 1977, 1979), the *Phobos 2* (Sagdeev and Zakharov, 1989), and the *Mars Express* (Chicarro et al., 2004) spacecraft.

5. Orbits and parameters

5.1. Revised orbits

We revised the orbits described in Jacobson (2010) by augmenting the observation set with Doppler tracking data from three *Mars Express* Phobos close flybys and additional *Mars Express* imaging observations of Deimos through 2011 (Pasewaldt et al., 2012) and by upgrading the dynamical model. The upgrades include the use of the latest planetary ephemerides (Folkner, 2011) and Martian gravity field and Mars orientation (Konopliv et al., 2011). In addition, we increased the Martian gravity field truncation from degree 8 to degree 10 in the zonal harmonics and from degree and order 5 to degree and order 6 in the tesseral harmonics (higher degree and order have sub-meter level effects on the integrated orbits). We also included the seasonal variation in third zonal harmonic due to the mass exchange between the Mars

polar caps and the force of the tide raised on Mars by the Sun (these have a negligible effect on the integration but are included for consistency with Konopliv's gravity field). We retained the Sun, Jupiter, Saturn, Earth, and Moon as the only perturbing bodies; the perturbations due to the remaining planets and the asteroids are not detectable in the observational data at this time. We continued to ignore the tides raised on the satellites (their effects are orders of magnitude smaller that those of the tides raised on Mars Szeto, 1983).

The integrated orbits were fit, in a weighted least-squares sense, to the full observational data set by adjusting the epoch position and velocity of each satellite, the Phobos tidal bulge lag angle, and the masses of Mars, Phobos, and Deimos. However, rather than estimating the Phobos libration amplitude, as was done for the previous orbit, we adopted the observed libration amplitude (Willner et al., 2010) and estimated the Phobos gravity field harmonics.

Since Phobos is in synchronous rotation (its rotation period matches its orbital period), the angle between the direction from Phobos to Mars and Phobos's axis of minimum principal moment of inertia is small and can be represented by $\theta = (2e + \mathcal{A})\ \sin\ M$, where e is Phobos's orbital eccentricity, M is the mean anomaly in its orbit, and $\mathcal{A}$ is the libration amplitude. The Phobos quadrupole acceleration depends upon the libration amplitude and the gravity harmonics. In the numerical integration the force on Mars exerted by the quadrupole, neglecting the Phobos obliquity (i.e., the Phobos pole is aligned with its orbit normal), is

$$\mathbf{F}_0 = \frac{3}{2}\mu_1\left(\frac{R^2}{\rho^4}\right)[(J_2 + 6C_{22}\ \cos\ 2\theta)\,\hat{\boldsymbol{\rho}} + 4C_{22}\ \sin\ 2\theta\,\hat{\mathbf{t}}]$$

where μ_1 is the Phobos GM (GM is the product of the Newtonian constant of gravitation G and the body's mass M), R is the Phobos equatorial radius, ρ is distance from Phobos to Mars, J_2 is second degree zonal harmonic of the Phobos gravity field, C_{22} is second degree and order tesseral harmonic of the Phobos gravity field, $\hat{\boldsymbol{\rho}}$ is the unit vector directed from Mars toward Phobos, and $\hat{\mathbf{t}}$ is the unit vector in the Phobos orbit plane normal to $\hat{\boldsymbol{\rho}}$ in the direction of Phobos's orbital motion. The reactive force acting on Phobos is

$$\mathbf{F}_1 = -\left(\frac{\mu_0}{\mu_1}\right)\mathbf{F}_0$$

with μ_0 being the GM of Mars. This force introduces both secular and periodic perturbations into Phobos's orbit. Because θ is small, it is clear from the above expressions that the forces are approximately proportional to the product of $\mathcal{A}$ and C_{22}. The observational data are sensitive only to the Phobos acceleration, consequently, it is not possible to obtain reasonable estimates for both the libration amplitude and gravity harmonics from the data fit. Moreover, because the force, for small θ, depends upon the sum of J_2 and C_{22} with a small periodic variation proportional to C_{22}, a separate determination of both harmonics is difficult. In our estimation process, we included a priori values for both harmonics derived from the Phobos uniform density moments of inertia given in Willner et al. (2010) with a priori uncertainties of 50% of the values. We obtained estimates of $J_2 = 0.1057 \pm 0.0067$ and $C_{22} = 0.0148 \pm 0.0004$ but with a correlation of 0.96 which indicates that the estimates are not really independent. Our J_2 is consistent with the value for a uniform density satellite, but our C_{22} is smaller. We must emphasize, however, that our values for the harmonics are dependent upon our model for the quadrupole acceleration and the measured libration amplitude.

The revised Phobos orbit differs little from the previous one; the biggest change is along the orbit but is less than 2 km within the 100 years from 1950 to 2050. The revised Deimos orbit exhibits a larger change, primarily in mean motion, which leads to roughly a 16 km along the orbit difference within the same 100 year time span.

A consequence of the new Deimos orbit is an altered encounter geometry during the *Viking* 2 flyby. The *Viking* 2 Doppler tracking is the primary source of information on the Deimos mass; the altered encounter yields a revised Deimos $GM = 0.962 \pm 0.028\ \mathrm{km}^3\ \mathrm{s}^{-2}$. Our estimate of the Phobos GM was unchanged from its previous value despite the addition of the *Mars Express* tracking, i.e., the additional data simply confirmed the earlier estimate. See Pätzold et al. (2014) for a comprehensive discussion of the determination of Phobos's mass.

The quality of the fit to all of the data is comparable to that achieved with the previous orbits; the Deimos orbit fits the new *Mars Express* data better than the quoted 1–3 km astrometric measurement accuracy.

5.2. Phobos mean longitude acceleration

In examining the observations from 1877 to 1941 Sharpless (1945) found that by including an acceleration term he improved his fit to the observed longitudes of Phobos but not Deimos; he commented, however, that this was not a definitive result. Wilkins (1966) made an attempt to confirm the acceleration but was unsuccessful. In a comment on the Wilkin's work P. Goldreich suggested that the effect of tides should be examined, but most astronomers discounted the possibility of tidal effects because it was thought that Phobos was too small to raise a tide that would cause the Sharpless acceleration. In his subsequent analyses, Wilkins (1967, 1968) continued to find that the data fits could not be improved by including a longitude acceleration. Wilkins (1970) concluded that the observation set (1877–1956) was inadequate to determine the acceleration but that, if it exists, it must be much smaller that Sharpless's value and is probably due to tides.

Sinclair (1972) also concluded that he could not determine a definitive acceleration. However, Shor (1975) finally found a well-determined value when he extended the data arc to 1973. Moreover, when he included the *Mariner* 9 observations with the Earthbased data, Sinclair (1978) obtained a longitude acceleration that was consistent with that found by Shor. Subsequently, all of the theories that were developed between 1982 and 1993 and were fit to both Earthbased and spacecraft data determined roughly the same value for the longitude acceleration.

Taking a different approach Bills et al. (2005) used the observation of a Phobos transit observed by the *Viking* 1 lander in 1977, the MOLA range measurement to Phobos in 1998, and 15 transits of the Phobos shadow across Mars seen by MOLA from 1999 to 2004 to estimate the Phobos longitude acceleration. From the acceleration he determined a set of Mars tidal parameters. Using a combination of the same MOLA transits and observations of the Phobos shadow on Mars made with the Mars Orbiter Camera (MOC), Rainey and Aharonson (2006) also obtained values for the acceleration and Mars tidal parameters.

When developing numerically integrated ephemerides, Lainey et al. (2007), Shishov (2008), Jacobson (2010), and this work all took into account the Phobos longitude acceleration. Shishov applied the acceleration as a correction to the Phobos longitude. The other integrations, on the other hand, included a tide model in their equations of motion and explicitly determined the tidal lag needed to produce the necessary acceleration. Those works explicitly confirmed that the observed acceleration can be produced by a tide raised by Phobos.

Table 1 provides a summary of the accelerations found by various authors. It is interesting to note that the original Sharpless value is about 50% larger than the recently determined values. Moreover, the values found using two high quality theories, Morley and Chapront-Touzé, and three integrations, Lainey, Jacobson, and this work are in complete agreement. Table 2 summarizes the Mars love

Table 1
Phobos secular acceleration (mdeg yr^{-2}).

Value	Reference
1.882 ± 0.171	Sharpless (1945)
Indeterm.	Wilkins (1967, 1968)
0.960 ± 0.160	Sinclair (1972)
1.427 ± 0.147	Shor (1975)
1.326 ± 0.118	Sinclair (1978)
1.774 ± 0.107	Duxbury and Callahan (1982)
1.192 ± 0.021	Ivanov et al. (1988)
1.240 ± 0.017	Jones et al. (1989)
1.237 ± 0.017	Sinclair (1989)
1.271 ± 0.036	Morley (1989a)
1.249 ± 0.018	Jacobson et al. (1989)
1.270 ± 0.008	Chapront-Touzé (1990a)
1.290 ± 0.010	Emelyanov et al. (1993)
1.367 ± 0.006	Bills et al. (2005)
1.334 ± 0.006	Rainey and Aharonson (2006)
1.270 ± 0.015	Lainey et al. (2007)
1.248 ± 0.016	Shishov (2008)
1.270 ± 0.003	Jacobson (2010)
1.273 ± 0.003	Current

Table 2
Mars tidal parameters.

κ_2	Q	γ	Reference
0.163 ± 0.056	85.6 ± 0.4	$0.^{\circ}3346 \pm 0.^{\circ}0014$	Bills et al. (2005)
0.153 ± 0.017	78.6 ± 0.8	$0.^{\circ}3645 \pm 0.^{\circ}0039$	Rainey and Aharonson (2006)
0.152 ± 0.009	79.9 ± 0.7	$0.^{\circ}3585 \pm 0.^{\circ}0031$	Lainey et al. (2007)
0.152 ± 0.009	82.8 ± 0.2	$0.^{\circ}3458 \pm 0.^{\circ}0009$	Jacobson (2010)
0.183 ± 0.009	99.5 ± 4.9	$0.^{\circ}2880 \pm 0.^{\circ}0142$	This work

numbers, κ_2, tidal bulge lag angles, γ, and the associated tidal quality factors, Q ($Q = \cot 2\gamma$). Bills et al. (2005) estimated the love number, Rainey and Aharonson (2006) took the love number from Yoder et al. (2003), and Lainey et al. (2007) and Jacobson (2010) use the love number from Konopliv et al. (2006). For our current work, the love number is that associated with our adopted Mars gravity field (Konopliv et al., 2011). Note that because our love number is larger than the others, we require a smaller lag angle to produce the observed acceleration. The factor Q is a measure of a tidally distorted body's departure from perfect elasticity. The factors determined from Phobos's longitude acceleration are compatible with proposed models for the Martian interior (Zarkov and Gudkova, 1997), a result which strengthens the consensus that the acceleration is due to the tide.

5.3. Phobos forced libration

The libration amplitude, $\mathcal{A}$, bears a direct relation to the satellite's principal moments of inertia, A, B, and C, which are of interest in developing models of the satellite's interior structure, i.e.

$$\mathcal{A} = \frac{6\,(\mathrm{B}-\mathrm{A})}{\mathrm{C}-3\,(\mathrm{B}-\mathrm{A})}$$

See Peale (1977) and Duxbury (1977) for theoretical discussions of the libration and the above expression for its amplitude. Note that there will be no libration for an axially symmetric body where A = B (when the obliquity is neglected). Borderies and Yoder (1990) carried out a theoretical study of the libration and its connection with the Phobos gravity field and orbital motion. As mentioned earlier, their model was incorporated in the Chapront-Touzé theory.

From an analysis of the Phobos imaging observations obtained by *Mariner 9*, Duxbury (1974) roughly estimated the libration amplitude. Combining the *Mariner 9* and *Viking* imaging, Duxbury (1989) improved the amplitude estimate. Willner et al. (2010) later determined an amplitude from the *Mars Express* imaging that was over a factor of three more accurate than Duxbury's. Jacobson (2010) included the libration in the model used for his numerically integrated orbit. He adopted the Phobos gravity field from Borderies and Yoder (1990) and estimated the libration amplitude as one of the parameters in his fit of the orbit to data. His determination, unlike those of Duxbury and Willner, was not based on direct observation but rather was inferred from the effect of the libration on the orbital motion. As stated earlier, for our revised orbits, we adopted Willner's amplitude and estimated the Phobos gravity field harmonics.

Table 3
Phobos libration amplitude (deg).

Value	Reference
3.	Duxbury (1974)
0.81 ± 0.5	Duxbury and Callahan (1989)
1.19	Borderies and Yoder (1990)
1.03 ± 0.22	Jacobson (2010)
1.20 ± 0.14	Willner et al. (2010)

Table 4
Planetocentric mean elements at 1950 January 1.0 (TDT) referred to the local Laplace planes.

Element	Phobos	Deimos
a (km)	9375	23 458
e	0.01511	0.00027
ϖ (deg)	357.266	280.942
λ (deg)	90.991	250.444
i (deg)	1.076	1.789
Ω (deg)	207.779	24.422
$\dot{\lambda}$ (deg day^{-1})	1128.844409	285.161887
s (deg yr^{-2})	1.273×10^{-3}	
$\dot{\varpi}$ (deg day^{-1})	0.435	0.018
$\dot{\Omega}$ (deg day^{-1})	−0.436	−0.018
α (deg)	317.671	316.657
δ (deg)	52.893	53.529
ϵ[a] (deg)	0.009	0.889

[a] Laplace plane tilt to the Mars equator.

Table 3 summarizes the results of the various forced amplitude determinations; the values are all in statistical agreement at a little over 1°.

5.4. Orbital elements

The precise orbits of the satellites have been computed using numerical integrations fit to the observations. These orbits can be roughly approximated by precessing planetocentric ellipses referred to the Laplace planes, i.e., the Struve theory. The elements of the ellipses representing the latest orbits appear in Table 4: they are: a – semimajor axis, e – eccentricity, ϖ – longitude of periapsis, λ – mean longitude, i – inclination to the Laplace plane, Ω – longitude of the ascending node on the Laplace plane. The ICRF right ascension and declination, α and δ, of the Laplace plane poles are also given in the table. The orbital longitudes are measured from the intersection of the Laplace plane with the ICRF reference plane. The longitude acceleration s of Phobos was taken into account in the determination of the elements as was the long period perturbation in the Deimos mean longitude (Born and Duxbury, 1975), $\Delta\lambda = 0.^{\circ}27 \sin(20.^{\circ}0 - \dot{\Omega}\, t)$. Within the 100 year time span from 1950 January 1 to 2050 January 1 the root-mean-square differences between Mars relative positions derived from the ellipses with the mean longitude corrections and the integrated orbit positions are about 8 km for Phobos and 25 km for Deimos.

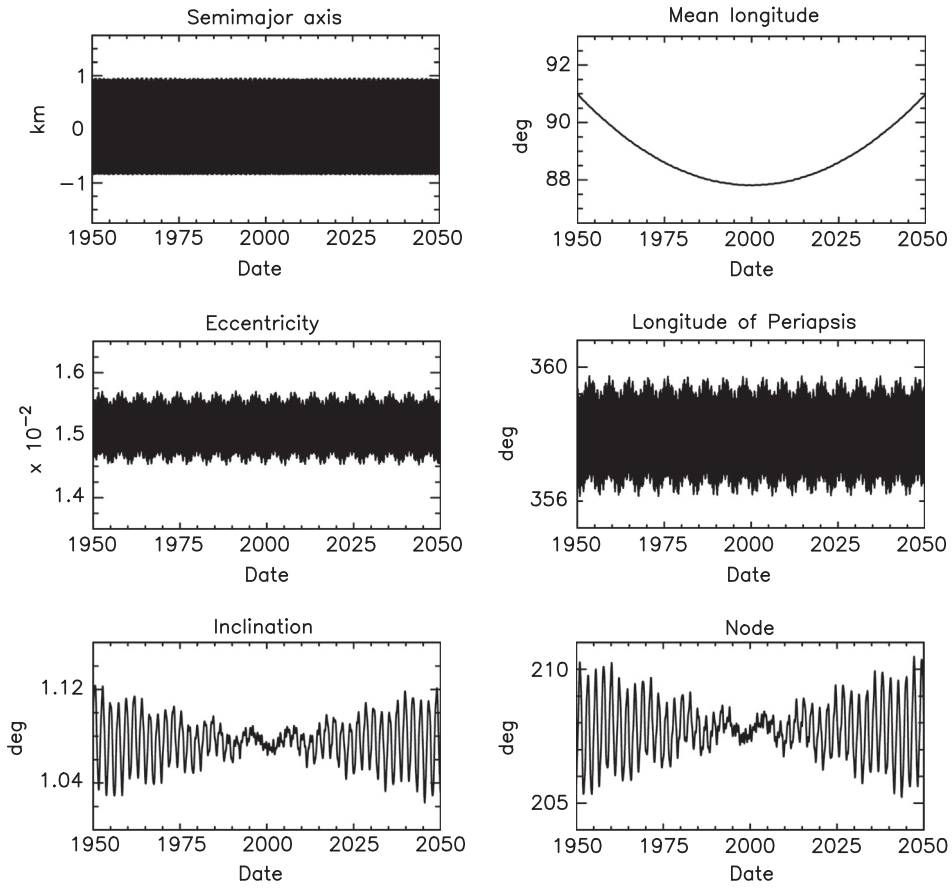

Fig. 2. Phobos osculating elements.

Figs. 2 and 3 display a history of the instantaneous osculating elements; the mean value of the semimajor axes and the secular changes in the longitudes and nodes have been removed. These elements were derived by converting the satellite positions and velocities from the latest numerically integrated orbits at each instant of time to elliptical orbital elements via the standard two-body motion transformations (Brouwer and Clemence, 1961). Clearly seen are the acceleration in the Phobos mean longitude and the long period perturbation in the Deimos mean longitude.

6. Future developments

6.1. Improving our current knowledge of the orbits

As shown many times in the past (e.g., Bell et al., 2005; Oberst et al., 2006), ephemerides tend to drift after some time. In particular, the fundamental frequencies of the system are never perfectly caught by the model, mostly because of observational error, and, though generally to a lesser extent, because of modelling assumptions. In practice, the error in the mean motion is the most significant because it induces a drift linear in time in the satellite orbit's mean longitude. Orbit errors tend to be smaller as the volume and time span of the observational data are increased. As a consequence, updated ephemerides are more accurate than older ones. Space missions normally require more accurate satellite ephemerides for specific experiments especially those relying on close flybys. Hence, there is always a need for ephemeris improvements over time.

The ephemerides may be improved by adding more new astrometric data or, alternatively, by improving old data. As previously discussed, new data these days are mostly gathered in space because of their much higher accuracy than ground based data. Hence, acquisition of new astrometric data mostly depends on the Mars missions and science teams interest in astrometry. On the other hand, reprocessing of old ground based observations may be done any time. In that regard, a new astrometric reduction of photographic plates used at the U.S. Naval Observatory covering the years 1969–1997 has recently been started (Robert et al., 2011). Benefiting from a modern scanning machine called DAMIAN (De Cuyper et al., 2012), all photographic plates from all observatories could be digitized with a high accuracy. Having digitized images allow the use of modern numerical techniques in the data reduction, and modern star catalogues can be introduced in the astrometric calibration. Measured positions of both Phobos and Deimos could significantly be improved by more than a factor of 3 (Robert et al., 2012). Moreover, the position of Mars itself versus stars in the field could be obtained. Completing this work for all relevant plates will require many years due to the large number of plates that have been used over the XXth century. Reprocessing old space images may also be of interest since star catalogues used in the 1970s were not as accurate as modern ones. This task is currently performed at JPL, as well as at Institut de Mécanique Céleste et de Calcul des Ephémérides (Thuillot et al., 2012).

6.2. Satellite orbits as a focus for future space missions

Because Martian satellite motions are significantly affected by their environment, their orbits can be used to probe the physics of the Martian system. In that respect, possessing a modern transmitter on the surface of one of these satellites would drastically improve our knowledge of its orbit. As a consequence, information on Mars' interior as well as that of Phobos or Deimos could be obtained. The PRIDE experiment on the *Phobos-Grunt* lander was

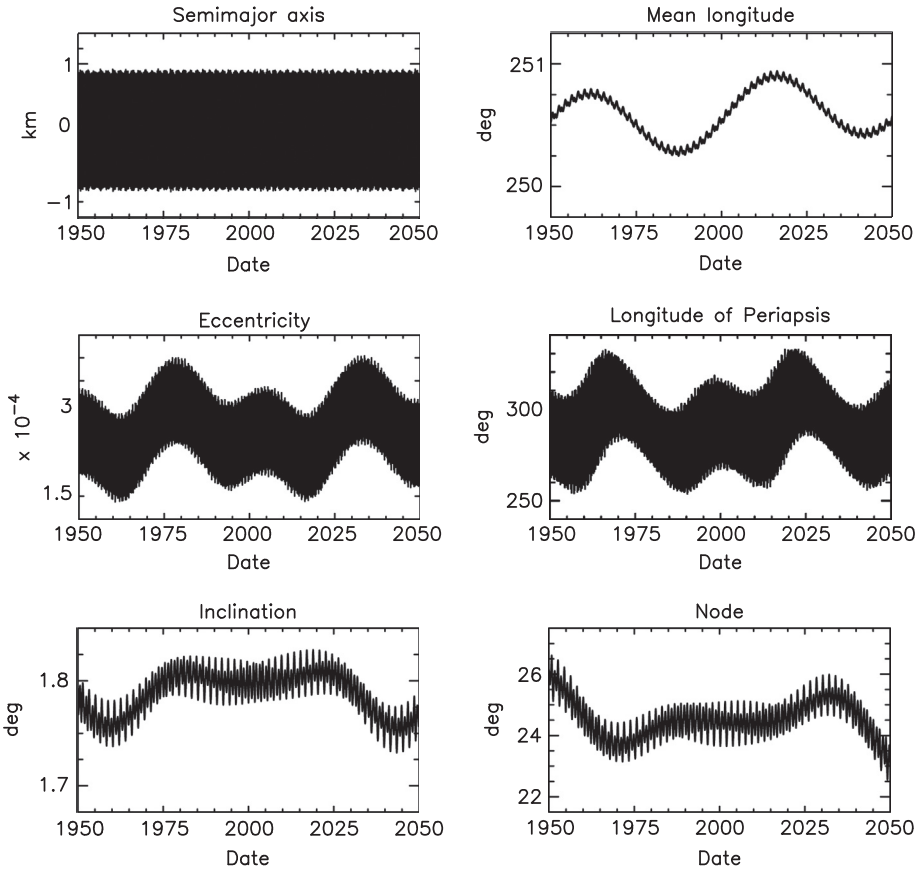

Fig. 3. Deimos osculating elements.

designed to track the Phobos motion over a year (Linkin et al., 2009). While the *Phobos-Grunt* mission unfortunately failed, a similar experiment has been selected for the *JUICE* mission to Jupiter with Ganymede as the main target.

General relativity may also be tested with the Phobos and Deimos orbits. Two space projects have included that as a goal. The first one, called *PLR* (for Phobos Laser Ranging), plans to perform a laser shoot from Phobos to the Earth. The expected quantification of the post-Newtonian parameter γ would be of two parts in 10^7. A second mission concept, called *GETEMME* (for Gravity, Einstein's Theory, and Exploration of the Martian Moons' Environment), proposes to perform a laser shoot between the two Martian satellites and a Mars spacecraft. Important results on both planetology and relativity tests are expected (Oberst et al., 2012).

7. Ephemerides

Ephemerides for the satellites based on the theories of Chapront-Touzé or Kudryavtsev and the integration of Lainey are available from Institut de Mécanique Céleste et de Calcul des Ephémérides (http://www.imcce.fr). Those from Jacobson's integration can be obtained from the On-Line Solar System Data Service at the Jet Propulsion Laboratory (http://ssd.jpl.nasa.gov) or from NASA's Navigation and Ancillary Information Facility (http://naif.jpl.nasa.gov).

8. Conclusions

In this paper we have examined the orbits of the Martian satellites, Phobos and Deimos. We reviewed the various representations of those orbits via analytical theory and direct numerical integration of their equations of motion. We also summarized the observational data, acquired from Earthbased observatories as well as from spacecraft, that have been used to determine the orbits. We presented the results of our latest least squares fit of our numerically integrated orbits to the data; within the context of those results, we discussed tidal acceleration and forced libration of Phobos. Finally, we commented on possible future developments.

Acknowledgment

The research described in this publication was carried out at the Jet Propulsion Laboratory, California Institute of Technology, under a contract with the National Aeronautics and Space Adminstration.

References

Akim, E.L., Stepanyants, V.A., Tuchin, A.G., Shishov, V.A., 2007. Motion Parameters Determination of the SC and Phobos in the Project Phobos-Grunt. Personal communication.

Aksnes, K., 1972. On the use of Hill variables in artificial satellite theory: Brouwer's theory. Astronomy & Astrophysics 17, 70–75.

Arlot, J.E., Emelyanov, N.V., 2009. The NSDB natural satellites astrometric database. Astronomy & Astrophysics 503, 631–638 ⟨http://lnfm1.sai.msu.ru/neb/nss/nssnsdcme.htm⟩.

Banerdt, W.B., Neumann, G.A., 2000. The Topography (and Ephemeris) of Phobos from MOLA Ranging. Technical Report, Jet Propulsion Lab California Institute of Technology, Pasadena, CA.

Bell, J.F., Lemmon, M.T., Duxbury, T.C., Hubbard, M.Y.H., Wolff, M.J., Squyres, S.W., Craig, L., Ludwinski, J.M., 2005. Solar eclipses of Phobos and Deimos observed from the surface of Mars. Nature 436, 55–57.

Bills, B.G., Neumann, G.A., Smith, D.E., Zuber, M.T., 2005. Improved estimate of tidal dissipation within Mars from MOLA observations of the shadow of Phobos. Journal of Geophysical Research 110, 1–15.

Borderies, N., Yoder, C.F., 1990. Phobos' gravity field and its influence on its orbit and physical librations. Astronomy & Astrophysics 233, 235–251.

Born, G.H., Duxbury, T.C., 1975. The motions of Phobos and Deimos from Mariner 9 TV data. Celestial Mechanics 12, 77–88.

Born, G.H., Tapley, B.D., 1969. An approximate solution for the short-term motion of a lunar satellite. Journal of Spacecraft and Rockets 6, 513–519.

Brouwer, D., 1959. Solution of the problem of artificial satellite theory without drag. Astronomical Journal 64, 378–397.

Brouwer, D., Clemence, G.M., 1961. Methods of Celestial Mechanics. Academic Press, NY and London.

Burton, H.E., 1929. Elements of the orbits of the satellites of Mars. Astronomical Journal 39, 155–164.

Chapront-Touzé, M., 1988. ESAPHO: a semi-analytical theory for the orbital motion of Phobos. Astronomy & Astrophysics 200, 255–268.

Chapront-Touzé, M., 1990a. Orbits of the Martian satellites from ESAPHO and ESADE theories. Astronomy & Astrophysics 240, 159–172.

Chapront-Touzé, M., 1990b. Phobos' physical libration and complements to the ESAPHO theory for the orbital motion of Phobos. Astronomy & Astrophysics 235, 447–458.

Chicarro, A., Martin, P., Trautner, R., 2004. The Mars Express mission: an overview. In: Wilson, A., Chicarro, A. (Eds.), Mars Express: The Scientific Payload, pp. 3–13.

De Cuyper, J., de Decker, G., Laux, U., Winter, L., Zacharias, N., 2012. The digitiser and archive facility at the ROB. In: Ballester, P., Egret, D., Lorente, N.P.F. (Eds.), Astronomical Data Analysis Software and Systems XXI, p. 315.

Duxbury, T.C., 1974. Phobos: control network analysis. Icarus 23, 290–299.

Duxbury, T.C., 1977. Phobos and Deimos: geodesy. In: Burns, J.A. (Ed.), Planetary Satellites. The University of Arizona Press, Tucson, AZ, pp. 346–362.

Duxbury, T.C., 1989. The figure of Phobos. Icarus 78, 169–180.

Duxbury, T.C., Callahan, J.D., 1982. The motions of Phobos and Deimos. In: Lunar and Planetary Institute Science Conference Abstracts, p. 191.

Duxbury, T.C., Callahan, J.D., 1988. Phobos and Deimos astrometric observations from Viking. Astronomy & Astrophysics 201, 169–176.

Duxbury, T.C., Callahan, J.D., 1989. Phobos and Deimos astrometric observations from Mariner 9. Astronomy & Astrophysics 216, 284–293.

Emelyanov, N.V., 1986. The construction of an analytical theory of artificial satellite motion with an accuracy up to third order with respect to the earth's oblateness. Astronomicheskii Zhurnal 63, 800–809.

Emelyanov, N.V., Nasonova, L.P., 1989. An analytical theory of the motion of Phobos and perturbation analysis. Astronomicheskii Zhurnal 66, 850–858.

Emelyanov, N.V., Vashkovyak, S.N., Nasonova, L.P., 1993. The dynamics of Martian satellites from observations. Astronomy & Astrophysics 267, 634–642.

Everhart, E., 1985. An efficient integrator that uses Gauss–Radau spacings. In: Carusi, A., Valsecchi, G.B. (Eds.), IAU Colloq. 83: Dynamics of Comets: Their Origin and Evolution. D. Reidel Pub. Co., Dordrecht, Holland, p. 185.

Folkner, W.M., 2011. Planetary Ephemeris DE424 for Mars Science Laboratory Early Cruise Navigation. Interoffice Memo. 343R-11-003 (Internal Document). Jet Propulsion Laboratory, Pasadena, CA.

Hartwell, J.G., 1967. Simultaneous integration of N-bodies by analytical continuation with recursively formed derivatives. Journal of the Astronautical Sciences 14, 173–177.

Ivanov, N.M., Kolyuka, Y.F., Kudryavtsev, S.M., Tikhonov, V.F., 1988. The theory of motion of Phobos—orbital parameters based on astrometric data and measurements taken aboard Mariner-9, and Viking-1, -2. Pis'ma Astronomicheskii Zhurnal 14, 956–960.

Jackson, J., 1924. Note on the numerical integration of $\frac{d^2x}{dt^2} = f(x,t)$. Monthly Notices of the Royal Astronomical Society 84, 602–606. (Origin of the Gauss–Jackson formula).

Jacobson, R.A., 2010. The orbits and masses of the Martian satellites and the libration of Phobos. Astronomical Journal 139, 668–679.

Jacobson, R.A., Synnott, S.P., Campbell, J.K., 1989. The orbits of the satellites of Mars from spacecraft and Earthbased observations. Astronomy & Astrophysics 225, 548–554.

Jones, D.P.H., Sinclair, A.T., Williams, I.P., 1989. Secular acceleration of Phobos confirmed from positions obtained on La Palma. Monthly Notices of the Royal Astronomical Society 237, 15–19.

Kolyuka, Y., Tikhonov, V., Polyakov, V., Avanesov, G., Heifetz, V., Zhukov, B., Akim, E., Stepanyants, V., Papkov, O., Duxbury, T., 1991a. Phobos and Deimos astrometric observations from the Phobos Mission. Astronomy & Astrophysics 244, 236–241.

Kolyuka, Y.F., Kudryavtsev, S.M., Tarasov, V.P., Tikonov, V.F., Ivanov, N.M., Polyakov, V.S., Potchukaev, V.N., Papkov, O.V., Sukhanov, K.G., Akim, E.L., Stephanians, V.A., Nasirov, R.R., 1991b. International project Phobos: experiment "Celestial Mechanics". Planetary and Space Science 39, 349–354.

Konopliv, A.S., Asmar, S.W., Folkner, W.M., Karatekin, O., Nunes, D.C., Smrekar, S.E., Yoder, C.F., Zuber, M.T., 2011. Mars high resolution gravity fields from MRO, Mars seasonal gravity, and other dynamical parameters. Icarus 211, 401–428.

Konopliv, A.S., Yoder, C.F., Standish, E.M., Yuan, D., Sjogren, W.L., 2006. A global solution for the Mars static and seasonal gravity, Mars orientation, Phobos and Deimos masses, and Mars ephemeris. Icarus 182, 23–50.

Kudryavtsev, S.M., 1993. Calculation of perturbations in the orbital elements of a nonspherical planet satellite in long-term intervals. In: Teles, J., Samii, M.V. (Eds.), Spaceflight Dynamics 1993. American Astronautical Society, Univelt, Inc., San Deigo, CA,
pp. 963–972. (AAS/GSFC International Symposium on Spaceflight Dynamics, Greenbelt, Maryland, 1993).

Lainey, V., Dehant, V., Pätzold, M., 2007. First numerical ephemerides of the Martian moons. Astronomy & Astrophysics 465, 1075–1084.

Lemoine, F.G., Smith, D.E., Rowlands, D.D., Zuber, M.T., Neumann, G.A., Chinn, D.S., Pavlis, D.E., 2001. An improved solution of the gravity field of Mars (GMM-2B) from Mars Global Surveyor. Journal of Geophysical Research 106, 23359–23376.

Linkin, V.M., Gotlib, V.M., Kosov, A.S., Strukov, I.A., Lipatov, A.N., Cimo, G., Gurvits, L. I., Pogrebenko, S.V., Turyshev, S.G., Kerzhanovich, V.V., 2009. Planetary radio interferometry and Doppler experiment with the Phobos-Grunt mission. In: European Planetary Science Congress, 2009, p. 376.

Morley, T.A., 1989a. A catalogue of ground-based observations of the Martian satellites 1877–1982. Astronomy and Astrophysics Supplement Series 77, 209–226.

Morley, T.A., 1989b. An improved determination of the orbits of the Martian satellites. In: Teles, J. (Ed.), Orbital Mechanics and Mission Design. American Astronautical Society, Univelt, Inc., San Deigo, CA, pp. 469–484. (Proceedings of an AAS/NASA International Symposium, April 1989, Goddard Space Flight Center).

Morley, T.A., 1990. An improved analytical model for the orbital motion of the Martian satellites. Astronomy and Astrophysics Supplement Series 228, 260.

Oberst, J., Lainey, V., Le Poncin-Lafitte, C., Dehant, V., Rosenblatt, P., Ulamec, S., Biele, J., Spurmann, J., Kahle, R., Klein, V., Schreiber, U., Schlicht, A., Rambaux, N., Laurent, P., Noyelles, B., Foulon, B., Zakharov, A., Gurvits, L., Uchaev, D., Murchie, S., Reed, C., Turyshev, S.G., Gil, J., Graziano, M., Willner, K., Wickhusen, K., Pasewaldt, A., Wählisch, M., Hoffmann, H., 2012. GETEMME—a mission to explore the Martian satellites and the fundamentals of solar system physics. Experimental Astronomy 34, 243–271.

Oberst, J., Matz, K.D., Roatsch, T., Giese, B., Hoffmann, H., Duxbury, T., Neukum, G., 2006. Astrometric observations of Phobos and Deimos with the SRC on Mars Express. Astronomy & Astrophysics 447, 1145–1151.

Pascu, D., Erard, S., Thuillot, W., Lainey, V., 2014. History of telescopic observations of the Martian satellites. Planetary and Space Science 102, 2–8.

Pasewaldt, A., Oberst, J., Wählisch, M., Willner, K., Hoffmann, H., Roatsch, T., Matz, K.D., Hussmann, H., 2011. New astrometric observations of Deimos with the SRC on Mars Express. In: EPSC-DPS Joint Meeting 2011, p. 558.

Pasewaldt, A., Oberst, J., Willner, K., Wählisch, M., Hoffmann, H., Matz, K.D., Roatsch, T., Hussmann, H., Lupovka, V., 2012. New astrometric observations of Deimos with the SRC on Mars Express. Astronomy & Astrophysics 545, A144.

Pätzold, M., Andert, T.P., Jacobson, R.A., Rosenblatt, P., Dehant, V., 2014. Phobos observed bulk properties. Planetary and Space Science 102, 86–94.

Peale, S.J., 1977. Rotation histories of the natural satellites. In: Burns, J.A. (Ed.), Planetary Satellites. The University of Arizona Press, Tucson, AZ, pp. 87–112.

Rainey, E.S.G., Aharonson, O., 2006. Estimate of tidal Q of Mars using MOC observations of the shadow of Phobos. In: Mackwell, S., Stansbery, E. (Eds.), 37th Annual Lunar and Planetary Science Conference, League City, TX, p. 2138 (Conference date: March 13–17, 2006).

Robert, V., de Cuyper, J.P., Arlot, J.E., de Decker, G., Guibert, J., Lainey, V., Pascu, D., Winter, L., Zacharias, N., 2011. A new astrometric reduction of photographic plates using the DAMIAN digitizer: improving the dynamics of the Jovian system. Monthly Notices of the Royal Astronomical Society 415, 701–708.

Robert, V., Pascu, D., Arlot, J.E., Lainey, V., 2012. A new reduction of USNO photographic plates of the Martian satellites. In: AAS/Division for Planetary Sciences Meeting Abstracts, p. #211.03.

Sagdeev, R.Z., Zakharov, A.V., 1989. Brief history of the Phobos mission. Nature 341, 581–587.

Seidelmann, P.K. (Ed.), 1992. Explanatory Supplement to the Astronomical Almanac. University Science Books, Mill Valley, CA.

Sharpless, B.P., 1945. Secular accelerations in the longitudes of the satellites of Mars. Astronomical Journal 51, 185–186.

Shishov, V.A., 2008. Determination of spacecraft and Phobos parameters of motion in the Phobos-Grunt project. Solar System Research 42, 319–328.

Shor, V.A., 1975. The motion of the Martian satellites. Celestial Mechanics 12, 61–75.

Sinclair, A.T., 1972. The motions of the satellites of Mars. Monthly Notices of the Royal Astronomical Society 155, 249.

Sinclair, A.T., 1978. The orbits of the satellites of Mars. Vistas in Astronomy 22, 133–140.

Sinclair, A.T., 1989. The orbits of the satellites of Mars determined from Earth-based and spacecraft observations. Astronomy & Astrophysics 230, 321–328.

Snyder, C.W., 1977. The missions of the Viking orbiters. Journal of Geophysical Research 83, 3971–3983.

Snyder, C.W., 1979. The extended mission of Viking. Journal of Geophysical Research 84, 7917–7933.

Struve, H., 1911. Uber die Lage der Marsachse und die Konstanten in Marssystem, Sitz. ber. Koniglich Preuss. Akad. der Wiss. fur 1911, 1056.

Synnott, S.P., 2007. Optical Navigation Technology Demonstration on MRO. Technical Report, D-37674, Jet Propulsion Laboratory, Pasadena, CA.

Szeto, A.M.K., 1983. Orbital evolution and origin of the Martian satellites. Icarus 55, 133–168.

Thomas, N., Britt, D.T., Herkenhoff, K.E., Murchie, S.L., Semenov, B., Keller, H.U., Smith, P.H., 1999. Observations of Phobos, Deimos, and bright stars with the imager for Mars Pathfinder. Journal of Geophysical Research 104, 9055–9068.

Thuillot, W., Lainey, V., Dehant, V., De Cuyper, J.P., Arlot, J.E., Gurvits, L., Hussmann, H., Oberst, J., Rosenblatt, P., Marty, J.C., Vermeersen, B., 2012. A new consortium: the European Satellite PArtnership for Computing Ephemerides (ESPaCE). In: Ballester, P., Egret, D., Lorente, N.P.F. (Eds.), Astronomical Data Analysis Software and Systems XXI, p. 659.

Tolson, R.H., Blackshear, W.T., Mason, M.L., 1977. The mass of Phobos. Geophysical Research Letters 4, 551–554.

Tyler, G.L., Balmino, G., Hinson, D.P., Sjogren, W.L., Smith, D.E., Woo, R., Armstrong, J.W., Flasar, F.M., Simpson, R.A., Asmar, S., Anabtawi, A., Priest, P., 2003. MGS-M-RSS-5-SDP-V1.0, in: Simpson, R.A. (Ed.), MGS RST Science Data Products. NASA Planetary Data System. USA_NASA_JPL_MORS_1021.

Wilkins, G.A., 1966. A new determination of the elements of the orbits of the satellites of Mars. In: Contopoulos, G. (Ed.), The Theory of Orbits in the Solar System and in Stellar Systems. D. Reidel, Dordrecht, Holland, pp. 271–273. (IAU Symposium 25).

Wilkins, G.A., 1967. The determination of the mass and oblateness of Mars from the orbits of its satellites. In: Runcorn, S.K. (Ed.), The Mantles of the Earth and Terrestrial Planets. Interscience, New York, pp. 77–84.
Wilkins, G.A., 1968. The analysis of the observations of the satellites of Mars. in: Colombo, G. (Ed.), Modern Questions of Celestial Mechanics. Edizione Cremoshese, Rome, pp. 221–240.
Wilkins, G.A., 1970. The problems of the satellites of Mars. In: Symposia Mathematica Istituto Nazionale di Matematica. Academic Press, London, pp. 29–43.
Wilkins, G.A., Springett, A.W. (Eds.), 1961. Explanatory Supplement to the Astronomical Ephemeris and the American Ephemeris and Nautical Almanac. Her Majesty's Stationery Office, London.
Willner, K., Oberst, J., Hussmann, H., Giese, B., Hoffmann, H., Matz, K.D., Roatsch, T., Duxbury, T., 2010. Phobos control point network, rotation, and shape. Earth and Planetary Science Letters 294, 541–546.
Willner, K., Oberst, J., Wählisch, M., Matz, K.D., Hoffmann, H., Roatsch, T., Jaumann, R., Mertens, V., 2008. New astrometric observations of Phobos with the SRC on Mars Express. Astronomy & Astrophysics 488, 361–364.
Wnuk, E., Breiter, S., 1992. The motion of natural and artificial satellites in Mars gravity field. Advances in Space Research 11, 183.
Yoder, C.F., Konopliv, A.S., Yuan, D.N., Standish, E.M., Folkner, W.M., 2003. Fluid core size of Mars from detection of the solar tide. Science 300, 299–303.
Zarkov, V.N., Gudkova, T.V., 1997. On the dissipative factor of the Martian interiors. Planetary and Space Science 45, 401–407.